ORNL/SPR-2023/3217

High Temperature Tensile Testing of Molybdenum Before and After Exposure in Flowing He at 600°C to 1000°C

Sebastien Dryepondt
Thomas Muth
Brandon Johnston
Charles Hawkins

January 2024

OAK RIDGE National Laboratory

ORNL IS MANAGED BY UT-BATTELLE LLC FOR THE US DEPARTMENT OF ENERGY

ORNL/SPR-2023/3217

Materials Science and Technology Division

HIGH TEMPERATURE TENSILE TESTING OF MOLYBDENUM BEFORE AND AFTER EXPOSURE IN FLOWING HE AT 600-1000°C

Author(s)

Sebastien Dryepondt
Thomas Muth
Brandon Johnston
Charles Hawkins

January 2024

Prepared by
OAK RIDGE NATIONAL LABORATORY
Oak Ridge, TN 37831
managed by
UT-BATTELLE LLC
for the
US DEPARTMENT OF ENERGY
under contract DE-AC05-00OR22725

CONTENTS

LIST OF FIGURES

ABSTRACT

ORNL supported NorthStar Medical Radioisotope's accelerator-based concept to produce the medical isotope molybdenum-99 (Mo-99). The Mo targets are expected to experience in the accelerator temperature ranging from 200°C to 1000°C, and previous studies have demonstrated the embrittlement of Mo targets at room temperature when exposed to impure He at 800 to 1000°C. The goal of this project was to evaluate potential embrittlement at temperature ranging from 600°C to 1000°C for three Mo materials exposed at the same temperatures for 100h in high purity He (O_2 <5ppm (µl/l)) with a flow rate of ~1m/s. Enriched Mo-100 (aMo) and conventional pressed and sintered Mo (UHP) disks were provided by NorthStar while low carbon arc cast rolled Mo, fabricated at ORNL, was used for comparison. The as fabricated rolled Mo exhibited superior tensile strength due to the alloy very fine grain size with limited ductility except at 1000°C with the elongation at rupture reaching 30%. The UHP Mo disks showed the lowest strength but highest ductility at 20-1000°C with significant strain hardening during tensile testing. The ductility of the aMo material was quite low at all temperatures due to a high density of voids at grain boundaries. Significant embrittlement of the aMo material was observed after exposure at 600°C to 1000°C, most likely because of oxygen diffusion and segregation at grain boundaries. No embrittlement was observed for the UHP Mo material, with excellent elongation at rupture for some of the specimens oxidized in He and tested at 600-1000°C. Significant variation in ductility from one UHP Mo specimen to another was, however, measured, both in the as fabricated and He-oxidized conditions. The rolled Mo was not affected by oxidation in He at 800°C, but a decrease in strength and increase in ductility was observed at 1000°C, likely due to the material recrystallization.

1. INTRODUCTION

Technetium-99m (Tc-99m), the decay product of Mo-99, is employed in the US in about two-thirds of isotope-based diagnostic medical procedures[1]. Historically, Mo-99 was produced by irradiating highly enriched uranium (HEU) targets in nuclear reactors. To limit nuclear proliferation, the National Nuclear Security Administration (NNSA)'s Mo-99 program started supporting projects looking at the HEU-free domestic production of Mo-99[2,3]. One of these projects is NorthStar's high energy electron-beam accelerator, aiming at Mo-99 production by exposing thin Mo-100 targets ~1inch in diameter for a week. To control the temperature of the irradiated targets, flowing helium is employed. However, even with flow rates superior to 50m/s, the target temperature is expected to vary from 200°C at the edges to >800°C in the center[4]. One key concern is the presence of impurities, in particular oxygen, in the He gas leading to target oxidation and degradation. Previous oxidation work conducted at 800°C and 1000°C on Mo commercial wrought sheet and Mo thin plates fabricated by powder metallurgy showed that concentration superior to 15ppm O_2 in flowing He at ~1m/s resulted in significant mass losses due to the growth and volatilization of an Mo oxide scale[5]. With an O_2 concentration of less than 5ppm, a very thin oxide scale was observed associated with very low mass changes after 100h at 1000°C.

The Mo target temperature gradient during irradiation might also lead to significant in-service thermal stresses, and the target tensile properties need to be considered. Unfortunately, oxidation of Mo might also result in oxygen ingress and Mo embrittlement. For example, Liu et al.[6] performed oxidation testing at 1150 °C in low pressure oxygen (1.3 mPa) on 0.51 mm thick Mo sheet for durations ranging from 100 h to 612 h and observed an increase of the ductile to brittle transition temperature (DBTT)from ~ -30°C[7] to ~200 °C. While the oxygen solubility in Mo is very low, less than 1 ppm[8], segregation/diffusion of oxygen at grain boundary can result in significant grain boundary embrittlement [6]. Interestingly, carbon also segregates at grain boundaries thus affecting oxygen segregation[9,10]. It is worth noting that several researchers have demonstrated the intrinsic brittle nature of specific Mo grain boundaries, even with very

low impurity contents[11,12]. Both the impurity content and the microstructure, in particular grain size and grain orientation, are highly dependent on the Mo sheet processing route[13,14,15]. For these reasons, small scale tensile testing was previously conducted at room temperature on both commercial and powder metallurgy Mo sheets, before and after exposure in flowing He with O_2 concentration varying from 0.5 to 5 ppm O_2 for 5 h to 100 h[16]. Exposure in flowing He with O_2 content varying from ~1 to 15 ppm O_2 at 1000 °C resulted in a decrease of the Mo wrought sheet strength and ductility, the longer the exposure time, the lower the ductility. Similar behavior was observed for the PM Mo materials but with a very low initial ductility for the as fabricated material leading to a very brittle behavior after high temperature exposure. The key objectives of this study was to evaluate the tensile behavior of enriched ^{100}Mo (aMo), pre-oxidized or not in impure He, at temperature up to 1000°C, and to compare the material properties with the properties of another powder metallurgy (PM) provided by NorthStar as well as low carbon arc cast Mo.

2. EXPERIMENTAL PROCEDURE

2.1 SPECIMEN CHARACTERIZATION

Specimens were cut using a low-speed saw, mounted in epoxy, and polished using colloidal silica for the final polishing step. Backscattered scanning electron microscopy (BSE-SEM) images and electron backscatter diffraction (EBSD) measurements were acquired using a Tescan Mira3 microscope. Fracture surface analysis of the specimens after tensile testing was conducted using an Hitachi 4800 SEM equipped with an energy dispersive X-ray spectroscopy (EDS) detector for chemical analysis.

2.1 MATERIALS

2.1.1 Powder Metallurgy disks

One-inch enriched ^{100}Mo (referred to as aMo in this report) and ultra-high purity (UHP) PM Mo disks, were provided by NorthStar. UHP refers to the ultra-high purity Ar used during the consolidation process of non-enriched Mo powder. The aMo disks were 0.5mm thick while the UHP disks were 0.7mm thick. While the exact fabrication procedure is considered proprietary, the fabrication approach was consistent with processing of Mo disks conducted at ORNL, described in previous reports[5], with powder sintering at 1600 °C for 4 h and an applied stress of 775 MPa.

BSE-SEM micrographs of the aMo and UHP Mo disks are presented in Figure 1. A much higher porosity density was observed for the aMo in comparison with the UHP Mo. In both cases, two populations of voids were observed, large voids at grain boundaries and smaller voids inside the grains. The very fine grain structure observed in Figure 1 for the aMo disk was confirmed by EBSD imaging. The EBSD maps in Figure 2 revealed an average grain size of 5um for the aMo disk and 21um for the UHP Mo, with no grain texture.

2.1.2 Low Carbon Arc Cast rolled Mo sheet

Arc cast melting allows for the fabrication of Mo with low oxygen content, but the process needs to be carefully controlled to avoid high carbon concentration. The ASTM B386 for low-carbon arc-cast (LCAC) molybdenum specifies concentration of <100wppm carbon and <15wppm oxygen[15]. A vacuum arc remelter was used to produce a low carbon Mo ingot 65 mm in diameter. The cast material was extruded into a bar ~20 mm x 50 mm and then machined and hot rolled to produce a plate ~6.3 mm thick. After homogenization at 1150°C for 1h, the plate was further warm rolled at 650°C to obtain a sheet ~0.63mm in thickness. As can be seen in Figure 2c, the fabrication process resulted in small textured grains elongated along the rolling direction.

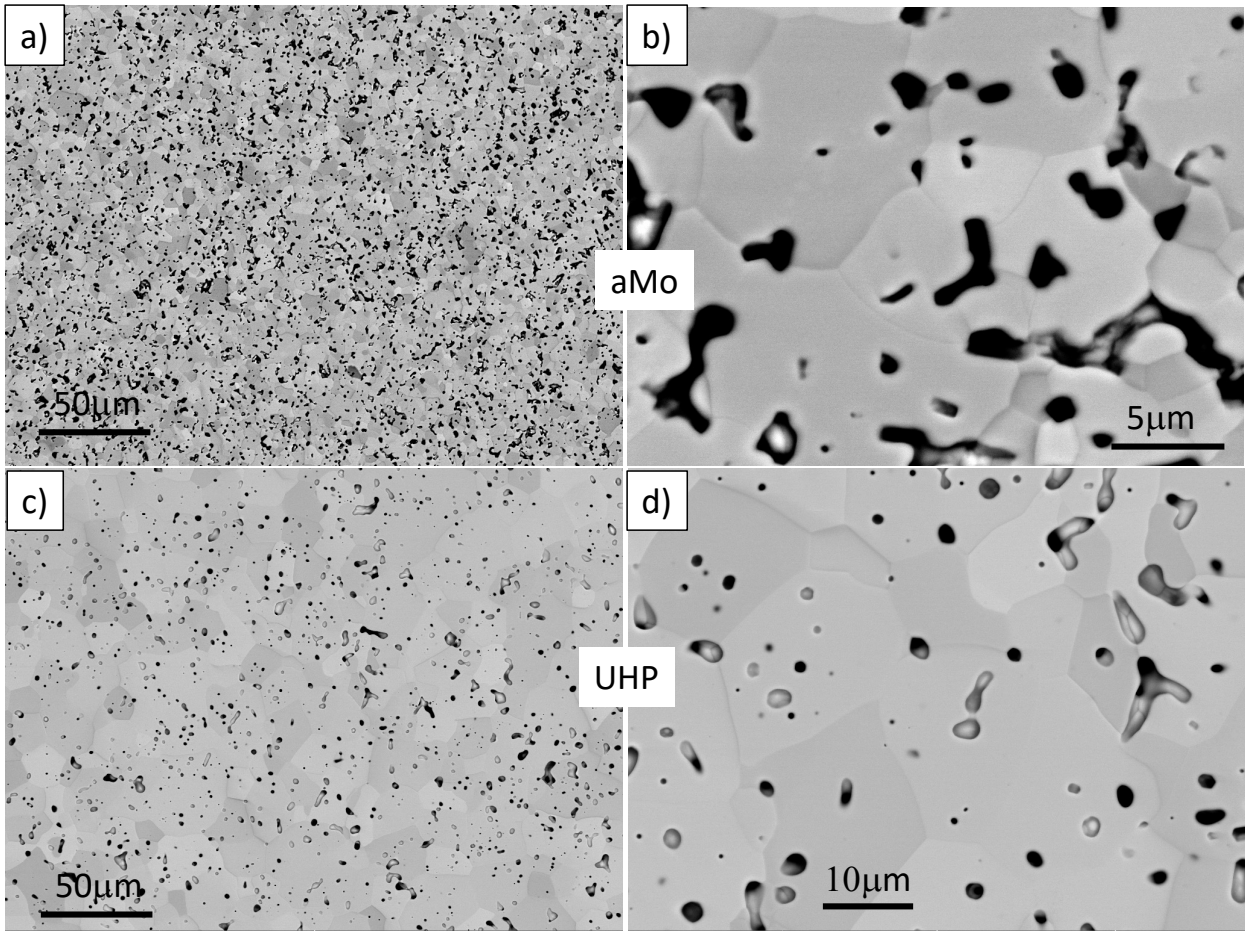

Figure 1:BSE-SEM micrographs of the PM materials, a) and b) aMo, c) and d) UHP Mo.

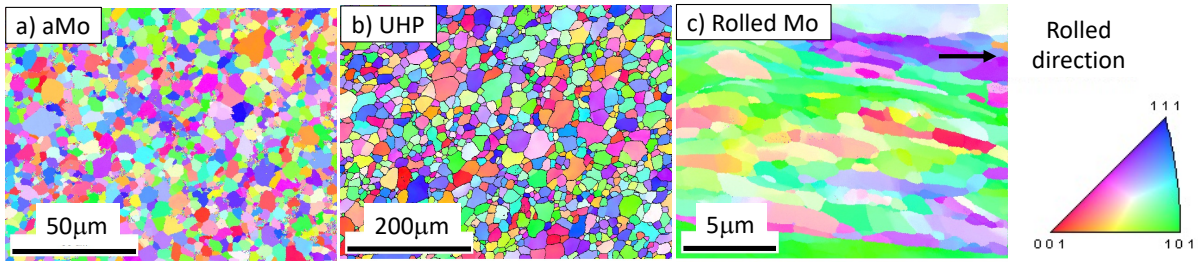

Figure 2: EBSD maps, a) aMo, b) UHP Mo and c) Rolled Mo.

2.2 TENSILE TESTING

As can be seen in Figure 3, small scale SS3 tensile specimens, 25.4mm long with a gage length of 7.62mm and a gage width of 1.5mm were machined by water jetting from the aMo and UHP Mo disks as well as the Mo rolled sheet. Three specimens could be machined from each disk and specimens were machined along and perpendicular to the rolled direction for the Mo rolled sheet. Tensile testing was conducted at 20°C, 600°C, 800°C and 1000°C at deformation rate of ~$10^{-3}s^{-1}$ with an MTS hydraulic frame or an Instron electro-mechanical machine. For the tests performed at high temperatures, flowing Ar

through an alumina chamber sealed with compressed high temperature insulation sheets was used to prevent oxidation during testing. Ta or Zr foils were also wrapped around the tensile grips to act as oxygen getters. Mass change measurement before and after testing confirmed that oxidation was negligible. The small size of the SS3 specimens did not permit the use of extensometers, and the yield strength, ultimate tensile strength and plastic deformation were estimated from the machine crosshead displacement. The tensile specimens were cleaned in ethanol and methanol prior to mechanical testing or exposure in flowing He and dimensions were measured using both a Keyence 3D microscope and a caliper.

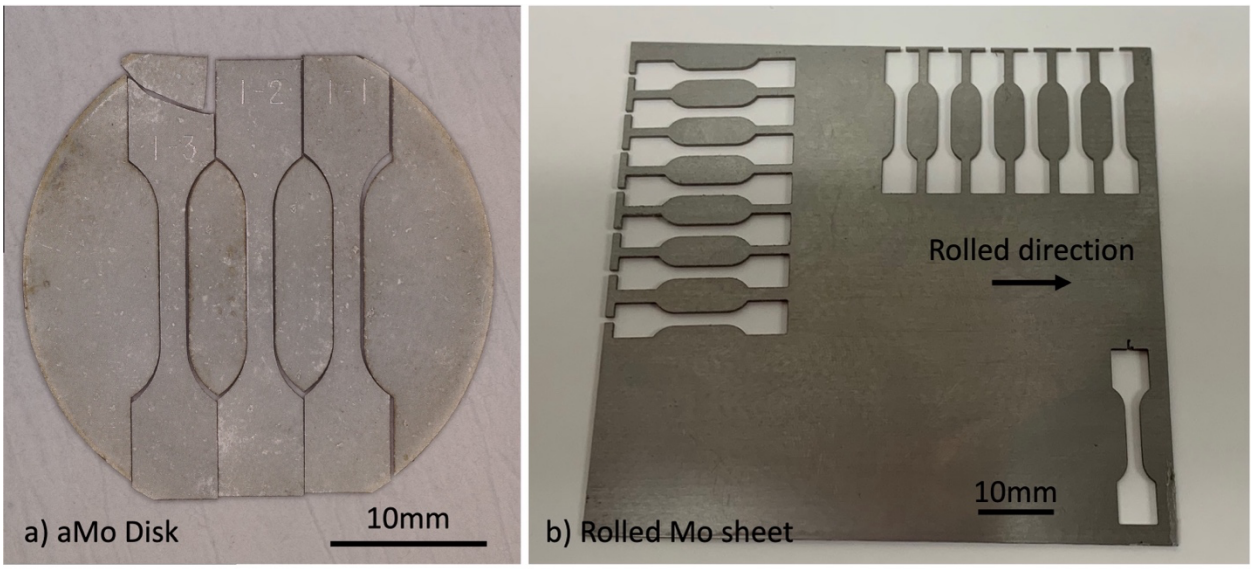

Figure 3: a) SS3 specimens machined from an aMo disk, b) Rolled Mo sheet showing locations of the machined SS3 specimens.

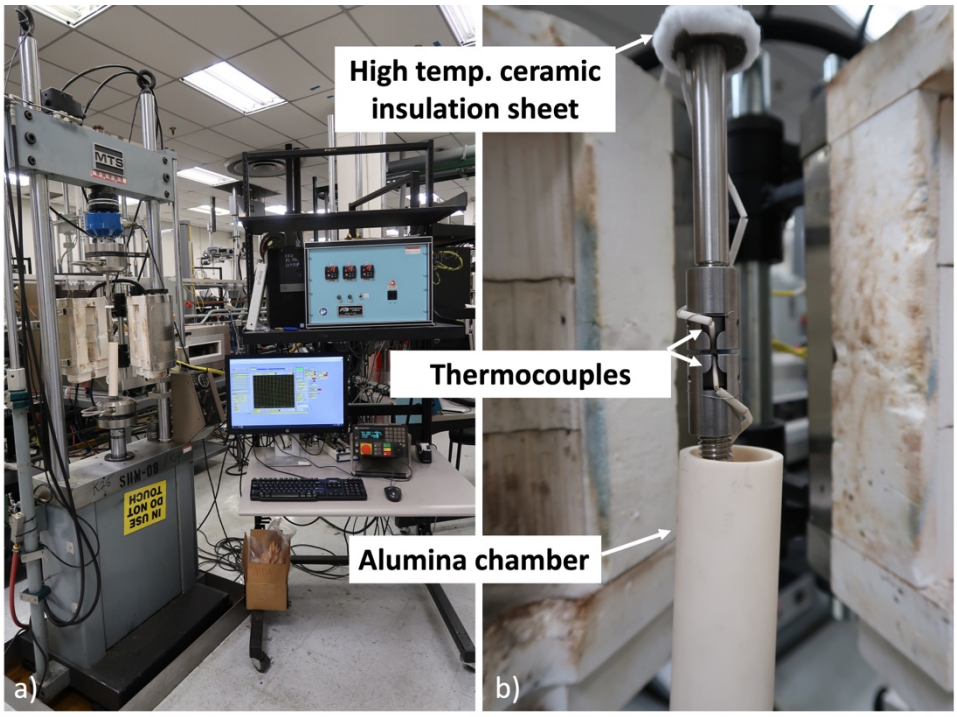

Figure 4: High temperature tensile testing in flowing Ar, a) overview of the testing systems, b) Thermocouples in contact with the specimen and alumina chamber and high temperature insulation sheet used to seal the system.

2.3 EXPOSURE IN FLOWING HELIUM AT 600-1000°C

The high temperature high flowing rate rig used to expose tensile specimens at 600°C, 800°C and 1000°C in flowing He has been described in detail elsewhere[5,16], and Figure 5 highlights key features of the system. A sealed quartz tube was inserted into a three-zone horizontal furnace whose temperature was calibrated before exposure. Specific quartz to stainless steel seals and copper gaskets were used to suppress any air ingress during testing. High purity He with a maximum O_2 concentration of 5ppm was flown through an alumina tube 0.63mm in diameter at 500 cm^3 /min to reach a flow rate of ~1m/s. A small grove in the alumina tube allowed insertion of the tensile specimens which were pinned using a small Pt wire. The O_2 content in the system was measured at the inlet and outlet of the system using GE oxy.IQ oxygen sensors. The specimens were exposed for 100h at the same temperature as the tensile testing temperature, i.e. 100h at 800°C before tensile testing at 800°C. These specimens are referred to as "oxidized" in the report.

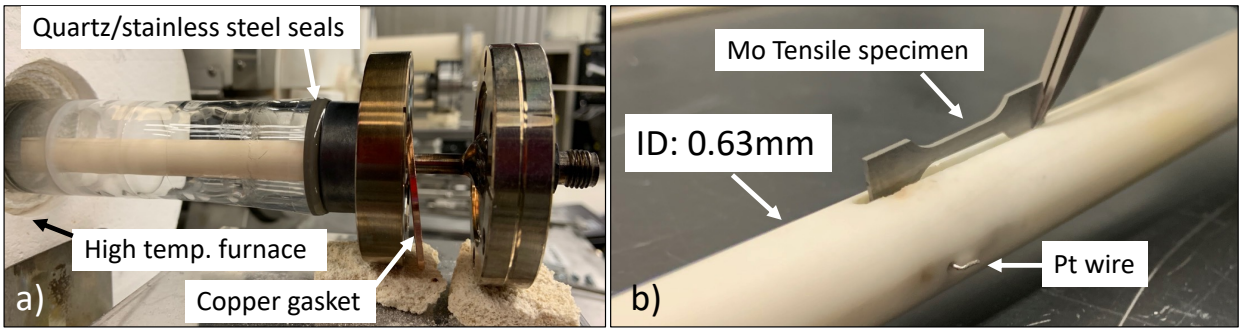

Figure 5 : High temperature testing in high flow rate He gas, a) sealed quartz tube to ensure precise control of the environment, b) Alumina tube with a small grove to insert Mo specimens.

3. RESULTS AND DISCUSSION

3.1 Tensile Results

Figure 6 shows the tensile curves obtained at 800°C and 1000°C for as fabricated and He oxidized specimens made of aMo, UHP Mo and rolled Mo. A quite different tensile behavior was observed for the three materials at 800°C. The rolled material exhibited much higher tensile strength but necking i.e. localization of the deformation was observed as soon as the ultimate tensile strength (UTS) was reached. Such high strength can be attributed to the material very small grain size and high dislocation after warm rolling. The tensile strength of the aMo material was significantly lower, with an unusual plastic deformation that has been previously attributed to the high pore density in the material, leading to crack propagation along voids[16]. The UHP Mo material exhibited even lower tensile strength, but significant hardening was observed, with an abrupted rupture after ~12% plastic deformation.

After oxidation in He at 800°C, the tensile behavior of the rolled Mo was unchanged while the aMo material showed a decrease of ductility. Surprisingly, the ductility of the UHP Mo specimen was significantly higher after oxidation in He, reaching a 42% plastic elongation at rupture.

Trends for the tensile behavior of the as fabricated Mo materials were similar at 1000°C, except for a significant ductility improvement for the rolled Mo and UHP Mo specimens. Oxidation for 100h in He at 1000°C led to a significant change of the rolled Mo tensile curve at 1000°C, with a notable decrease in strength and increase in ductility due to a less pronounced localization of the deformation. This change is likely due to recrystallization during the exposure for 100h at 1000°C as reported by Cockeram et al[17].

For the aMo specimen, oxidation in He for 100h at 1000°C led to a very brittle behavior with no plastic deformation, as has been observed for specimens tested at room temperature after oxidation in He at 1000°C[16]. Finally, oxidation in He for 100h at 1000°C for the UHP Mo resulted in a significant decrease in ductility, contrary to what was observed at 800°C.

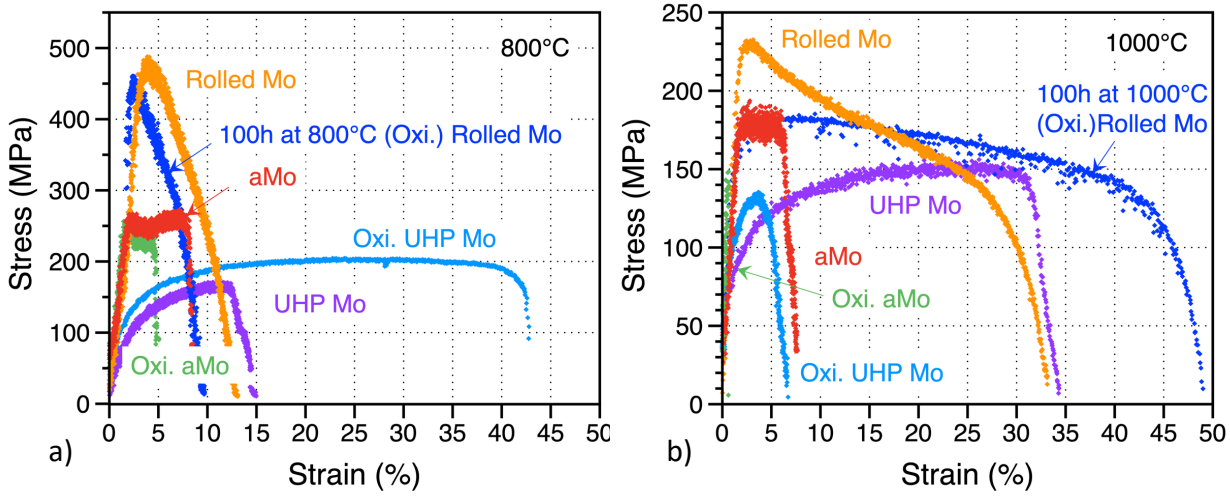

Figure 6: Tensile curves for the as fabricated and He oxidized aMo, UHP Mo and rolled Mo specimens, a) 800°C and b) 1000°C.

Table 1 and Table 2 summarize all the tensile results from 20°C to 1000°C for the powder-based Mo and rolled Mo materials, respectively, and Figure 7 highlights the evolution with temperature of the yield strength, UTS and plastic deformation for these Mo materials. All the rolled Mo results presented in Figure 7 were obtained with specimens machined perpendicular to the rolled direction. As stated in Table 1, some aMo and UHP Mo specimens failed during test preparation. The strength of these specimens could not be assessed but a plastic deformation of 0% was assumed due to the very brittle nature of the specimen rupture. Figure 7a, focused on the as fabricated strength, highlights again the superior strength of the rolled Mo in comparison with the two powder-based Mo materials, but the rolled material exhibited a more noticeable decrease in strength with increasing temperature. The larger difference between the yield and UTS for the UHP Mo specimens at all temperatures confirmed the significant hardening of the alloy observed in Figure 6. Figure 7b shows higher elongation at rupture for the UHP Mo specimen, except for the one specimen that failed during specimen preparation. The rolled Mo exhibited plastic deformation of ~7 to 10% from 20°C to 800°C with a drastic increase at 1000°C.

Figure 7c compares the UTS of the three Mo materials before and after He exposure. None of them was significantly impacted by exposure in He, with only a slight UTS decrease for the aMo and rolled materials at 1000°C. As previously noted, the elongation at rupture for the rolled Mo was unchanged after oxidation in He at 800°C but increased at 1000°C, while the ductility of the aMo disks decreased after oxidation in He at 600°C, 800°C and 1000°C. Results for the He-oxidized UHP Mo specimens were quite surprising, with high ductility measured at 600°C and 800°C but low ductility measured at 1000°C. These results are likely due to a significant variation in the ductility of the UHP Mo specimens from one specimen to another rather than an effect of oxidation in He between 600°C and 1000°C. It is worth noting that specimens exhibiting very different elongation at rupture were machined from the same disks (Table 1).

Table 1: Summary of the tensile tests conducted on aMo and UHP Mo disks.

Material	Gas	Exposure	Test Temp. (°C)	Disk	Position	Yield	UTS	Plastic Deformation
aMo	NA	As received	1000	220419_2	Center	179	193.6	6.4
aMo	NA	As received	1000	220419_2	Edge	fracture during set up		
aMo	NA	As received	800	220419_2	Edge	252	267	7.3
aMo	NA	As received	600	220101_50	Edge	258.5	287	10.4
aMo	NA	As received	20	220419_1	Edge	470	483	0.9
aMo	NA	As received	20	220419_1	Edge	485	496	0
aMo	HP <5ppm	100h 1000°C	20	220419_1	Center	fracture during set up		
aMo	HP <5ppm	100h 1000°C	1000	220101_50	Center	148	148	0
aMo	HP <5ppm	100h 800°C	800	220419_4	Edge	fracture during set up		
aMo	HP <5ppm	100h 800°C	800	220419_3	Center	238	256	4.1
aMo	HP <5ppm	100h 600°C	600	220101_50	Edge	243	283	5.5
UHP	NA	As received	1000	221102_18	Edge	82.7	136.6	33
UHP	NA	As received	800	221102_19	Center	103	172.8	11.4
UHP	NA	As received	800	221102_17	Edge	fracture during set up		
UHP	NA	As received	600	221102_19_3	Edge	127.5	225	18.7
UHP	NA	As received	20	221102_18	Edge	339	452	8.6
UHP	NA	As received	20	221102_17	Edge	345	489.2	15.9
UHP	HP <5ppm	100h 1000C	1000	221102_18	Center	99	135.3	5.2
UHP	HP <5ppm	100h 800C	800	221102_17	Center	121	207	40
UHP	HP <5ppm	100h 600C	600	221102_19	Edge	189.5	255	41.5

HP: high purity He, NA: Not applicable

Table 2: Summary of the tensile tests performed on rolled Mo.

Material	Exposure	Duration	Test Temp. (°C)	Direction	Yield	UTS	Plastic Deformation	Specimen
Rolled Mo	NA	As received	1000	Perpendicular to rolled dir.	242	242	32.9	MoRP_2
Rolled Mo	NA	As received	800	Perpendicular to rolled dir.	462	488	10	MoRP_3
Rolled Mo	NA	As received	400	Perpendicular to rolled dir.	710	751	6.8	MoRP_4
Rolled Mo	NA	As received	20	Perpendicular to rolled dir.	856.3	925	7.3	MoRP_1
Rolled Mo	HP <5ppm	100h 1000C	1000	Perpendicular to rolled dir.	159	198	48	MoRP_5
Rolled Mo	HP <5ppm	100h 800C	800	Perpendicular to rolled dir.	484	484	7.5	MoRP_6
Rolled Mo	NA	As received	20	Along rolled dir.	833.8	876.7	9.4	MoRL1
Rolled Mo	NA	As received	20	Along rolled dir.	845.5	890.5	9.2	MoRL2
Rolled Mo	HP <5ppm	100h 800C	800	Along rolled dir.	443	443	15	MoRL3

HP: high purity He, NA: Not applicable

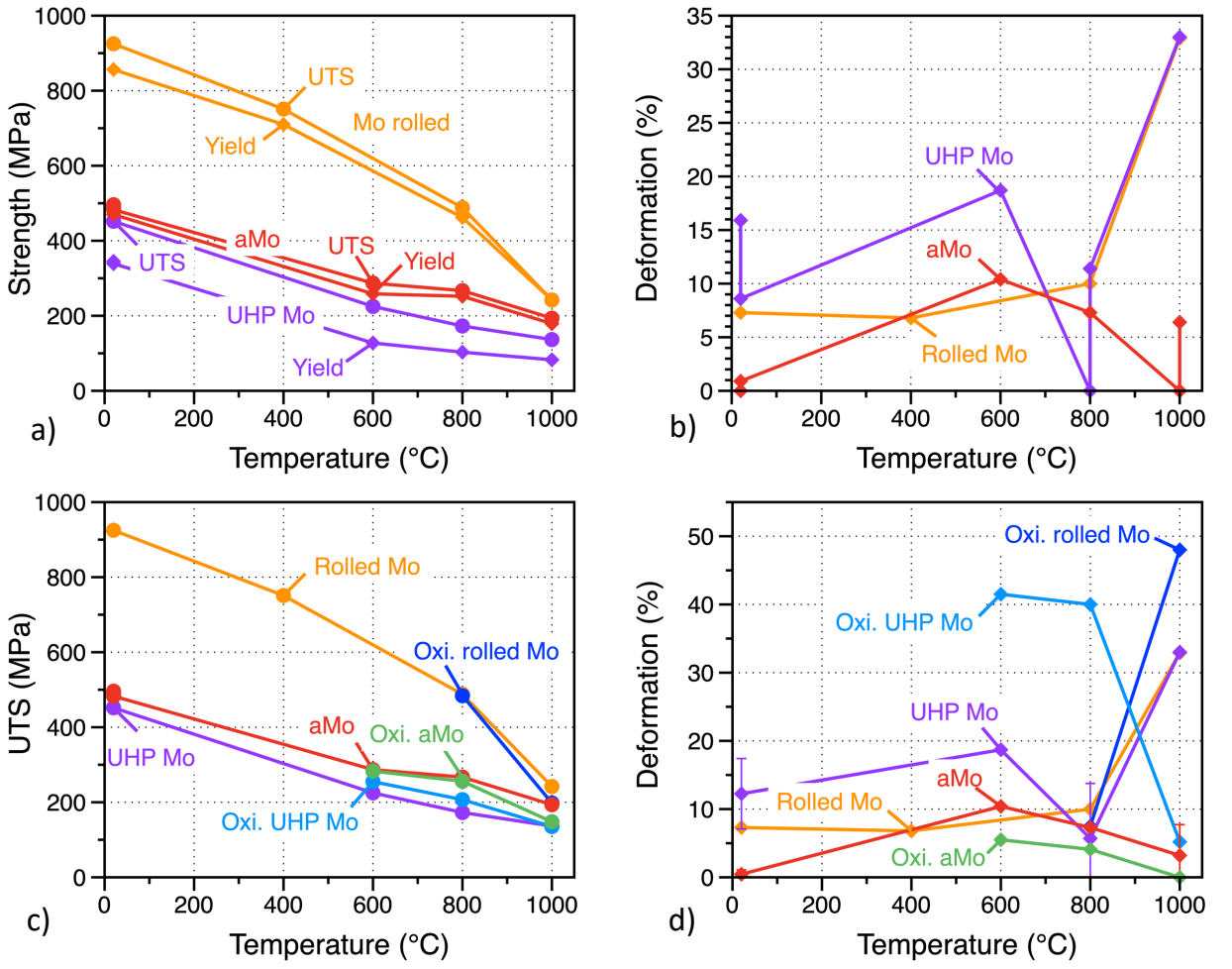

Figure 7: Tensile properties from 20°C to 1000°C for the aMo, UHP Mo and rolled Mo materials, a) as fabricated strength, b) as fabricated plastic deformation, c) strength comparison before and after exposure in He, d) ductility comparison before and after exposure in He. Note that data was averaged in d).

3.2 Microstructure characterization

The fracture surface of selected specimens was characterized by SEM, and representative micrographs are displayed in Figure 8 to Figure 10. As can be seen in Figure 8, brittle fracture surfaces were observed for all the aMo specimens tested at 800°C or 1000°C. Local inhomogeneity in the microstructure was observed in some specimens, as illustrated in Figure 8c. At higher magnification i.e. Figure 8, oxidation can be observed at the surface of some specimens, which likely took place after rupture in (impure) Ar (Figure 8f). It was previously reported that Mo oxides were observed at the fracture surface of aMo specimens tested at room temperature after oxidation in He at 1000°C[16]. The presence of these oxides confirmed oxygen segregation at grain boundaries leading to aMo embrittlement. Unfortunately, oxidation in impure Ar during tensile testing at 800°C or 1000°C prevented analysis of the oxidation taking place during exposure in He before tensile testing.

The fracture surfaces for the UHP Mo specimens (Figure 9) were much more heterogeneous, with the presence of crevasses of different sizes, with large crevasses only observed in low ductility specimens (Figure 9a and 9e). Quite ductile features were observed (Figure 9c) except at the bottom of these crevasses (Figure 9f). Finally, very different fracture surfaces were observed for the rolled Mo specimens (Figure 10), with extreme necking observed for most of the specimens tested at 800 and 1000°C. The specimen tested at 1000°C exhibited a very flat fracture surface, very different from the fracture surface of the other specimens. Further investigation is needed to understand the reason for this surprising result, since the curve in Figure 6b shows significant necking for all the rolled Mo specimens.

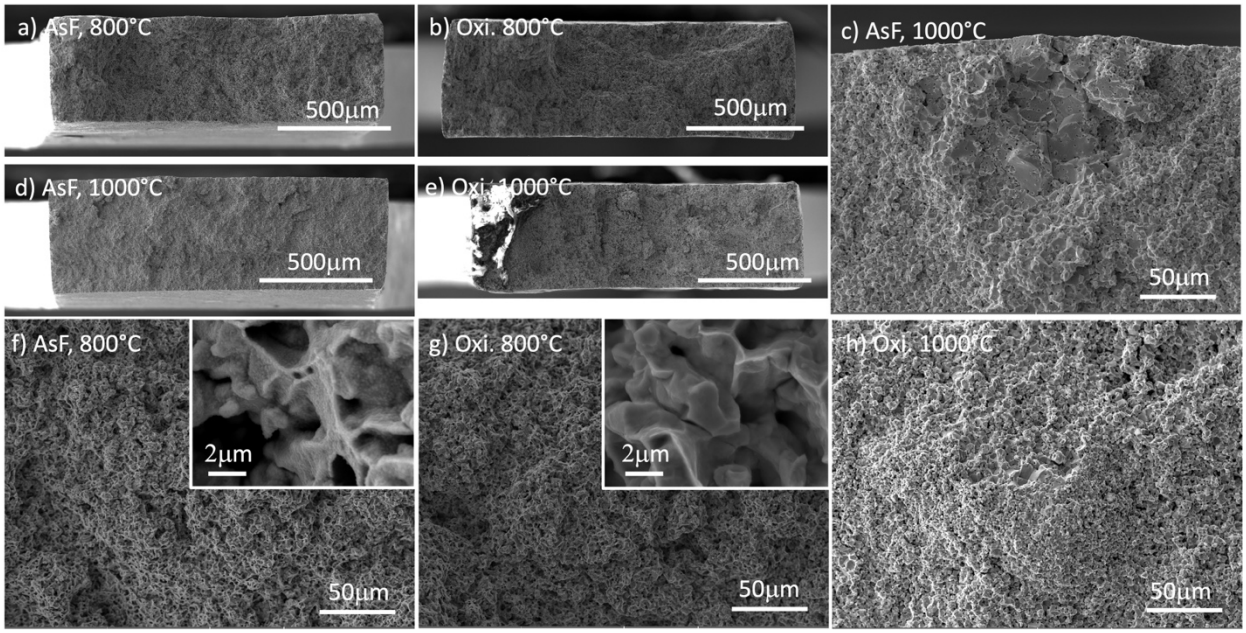

Figure 8: SEM micrographs of aMo fracture surfaces, a) and f) as fabricated aMo tested at 800°C, b) and g) specimen exposed in He and tested at 800°C, c) and d) as fabricated aMo tested at 1000°C, e) and h) specimen exposed in He and tested at 1000°C.

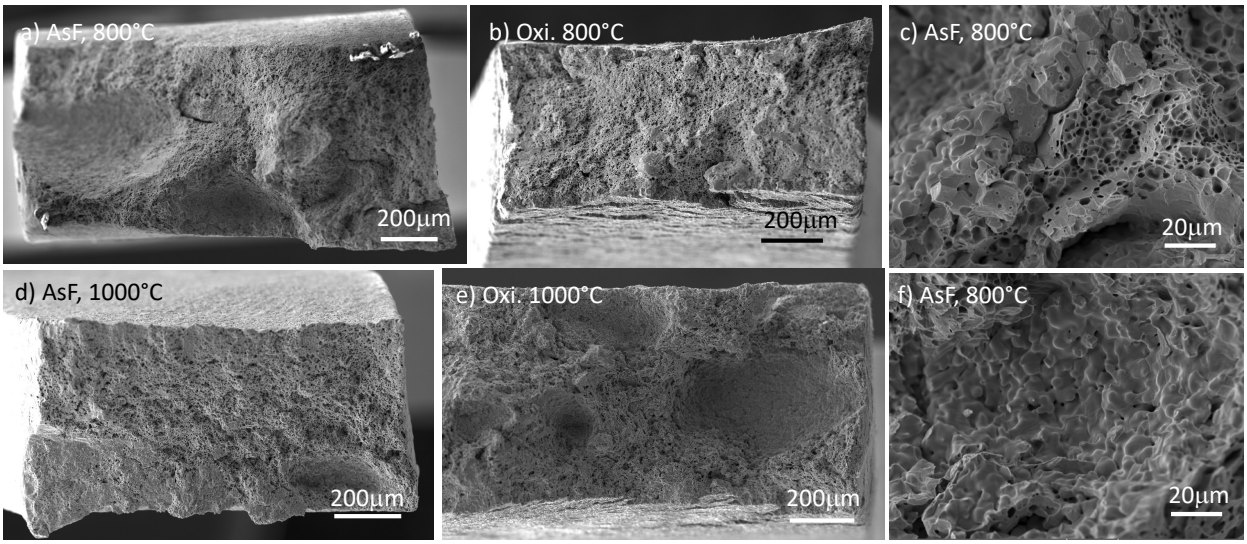

Figure 9: SEM micrographs of UHP Mo fracture surfaces, a), c) and f) as fabricated UHP Mo tested at 800°C, b) specimen exposed in He and tested at 800°C, d) as fabricated UHP Mo tested at 1000°C, e) specimen exposed in He and tested at 1000°C.

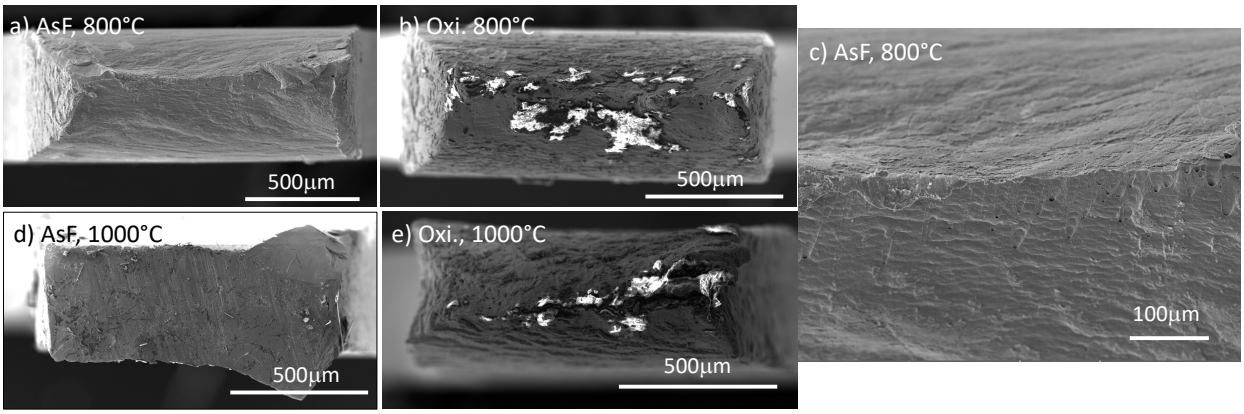

Figure 10: SEM micrographs of rolled Mo fracture surfaces, a) and c) as fabricated rolled Mo tested at 800°C, b) specimen exposed in He and tested at 800°C, d) as fabricated rolled Mo tested at 1000°C, e) specimen exposed in He and tested at 1000°C.

Cross-section micrographs of the aMo material are presented in Figure 11 and Figure 12 for the as fabricated and He-oxidized specimens, respectively. The microstructure of the as fabricated specimens tested at 800°C and 1000°C looks very similar to the initial microstructure in Figure 1, highlighting the limited impact of the exposure for ~20min at high temperature. The large field of view in Figure 11a and Figure 11c revealed local variation in defect density, while high magnification images in Figure 11b and Figure 11d highlight small cracks at grain boundaries often linked to the presence of voids. These observations indicate that the large void volume fraction at grain boundaries is the likely reason for the low ductility of the aMo material.

As can be seen in Figure 12, microstructures in the bulk of the aMo specimens exposed in He for 100h at 800°C and 1000°C before tensile testing were very similar, with voids and cracks at grain boundaries. The key difference was the presence of an Mo oxide scale at the specimen surface, ~2 micrometers thick at 800°C and ~5 micrometers thick at 1000°C. Embrittlement of the aMo material after exposure in

impure He at 800 and 1000°C was previously attributed to the likely diffusion and segregation of oxygen along grain boundaries[16].

Similar characterization was conducted on the UHP Mo specimens tested at 800 and 1000°C, and the resulting micrographs are shown Figure 13 and Figure 14, in the as fabricated and oxidized condition, respectively. For the as fabricated specimens and the specimen exposed for 100h at 1000°C in He, the microstructures were very similar to the initial microstructure presented in Figure 1c and Figure 1d, with voids observed both in the grain and at grain boundaries. The specimen exposed for 100h at 800°C exhibited a quite different microstructure, with significant void deformation along the load direction and the presence of multiple small cracks at the specimen surface. These features are consistent with the large deformation measured during tensile testing. This is a quite compelling result, demonstrating that high ductility can be obtained for powder-based Mo material. The reason for the drastic variation in ductility from one UHP Mo specimen to another is unclear and likely related to variability in microstructure. Based on the UHP Mo tensile curves, this variation is related to sudden necking for some specimens and could be linked to local defects or heterogeneous microstructures.

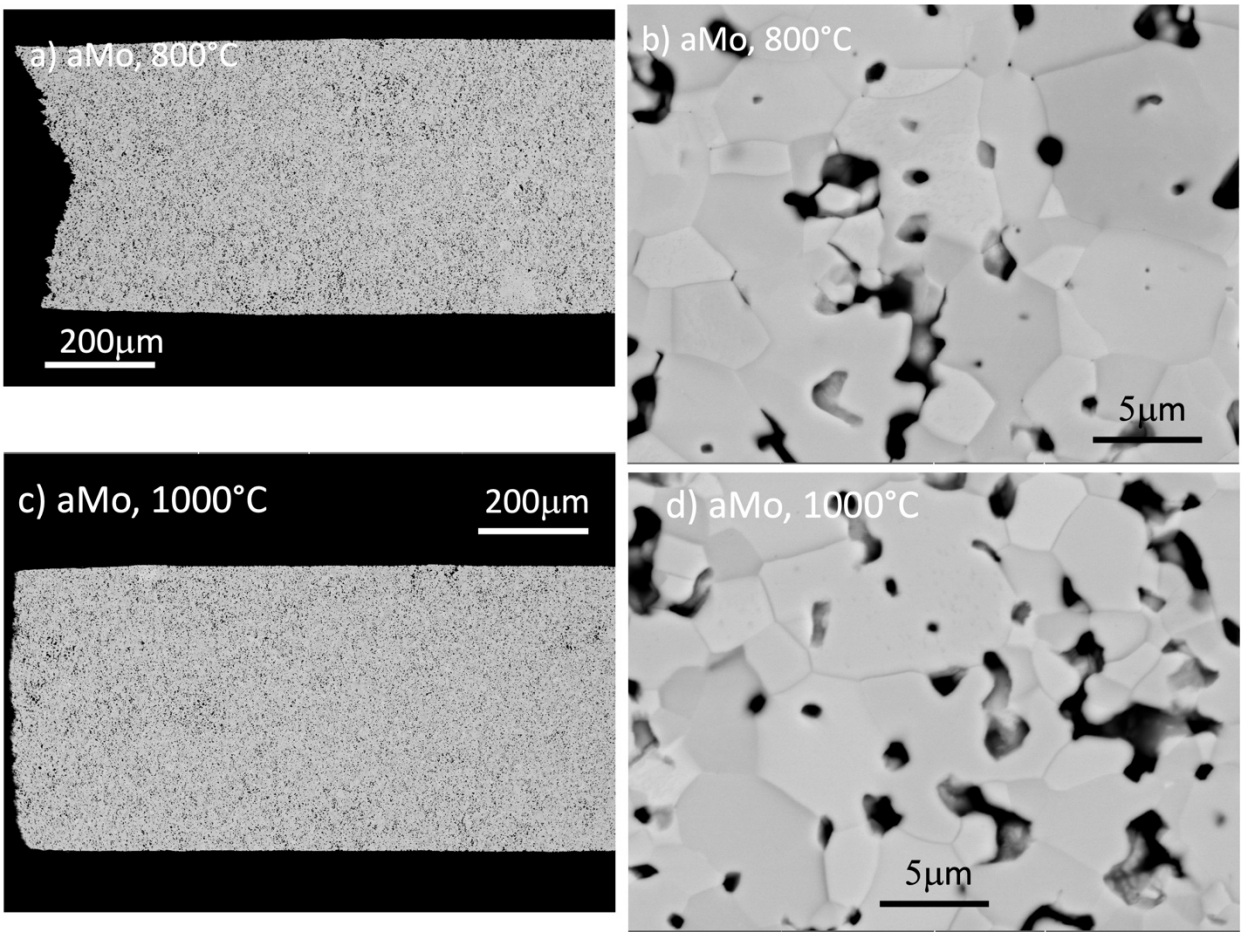

Figure 11: SEM cross section micrographs of the as fabricated aMo specimens, a) and b) tested at 800°C, c) and d) tested at 1000°C.

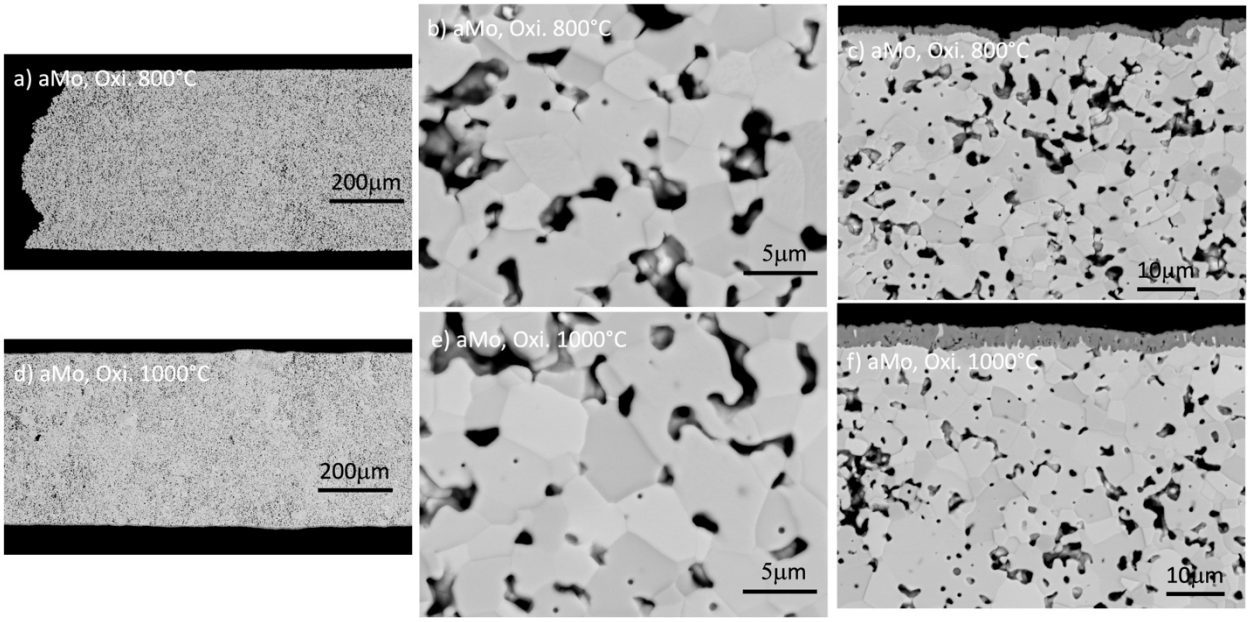

Figure 12: SEM cross-section micrographs of the aMo specimens exposed in He for 100h, a) through c) exposed and tested at 800°C, d) through f) exposed and tested at 1000°C.

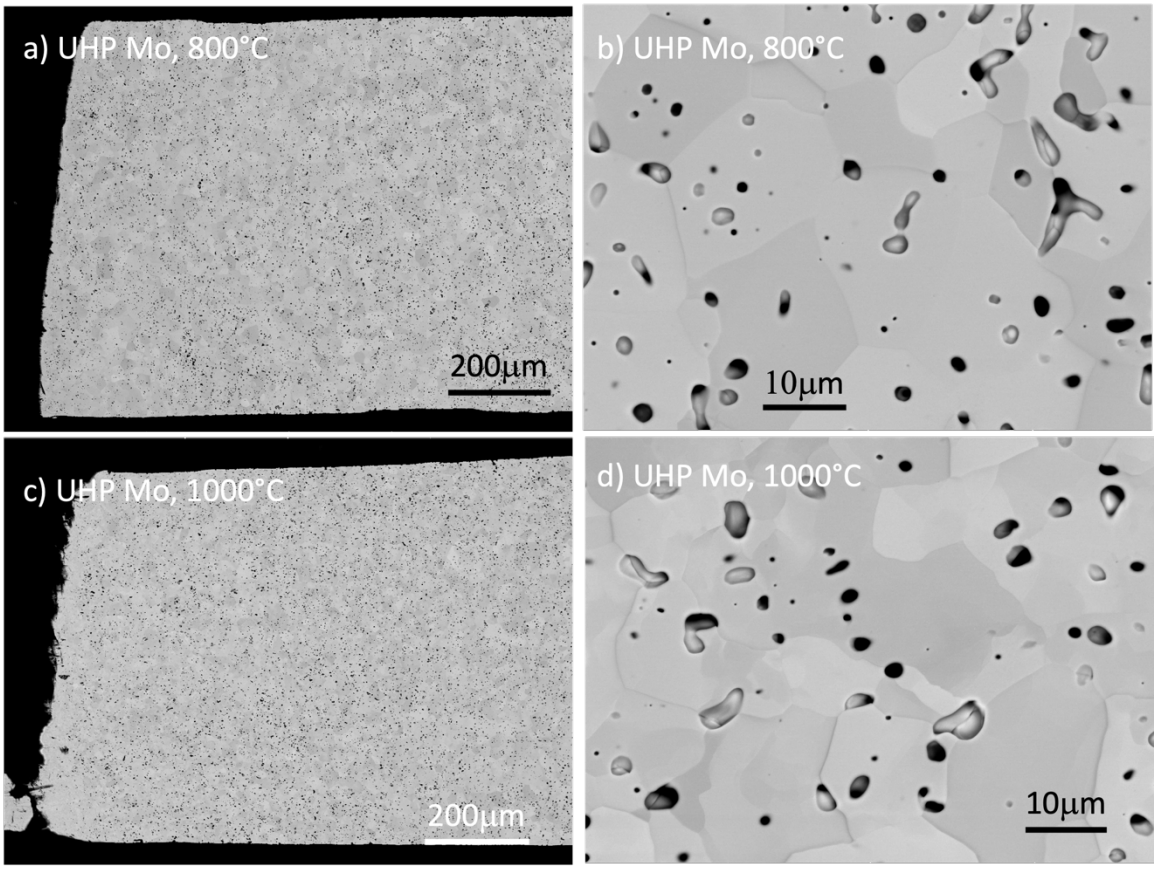

Figure 13: SEM cross section micrographs of the as fabricated UHP Mo specimens, a) and b) tested at 800°C, c) and d) tested at 1000°C.

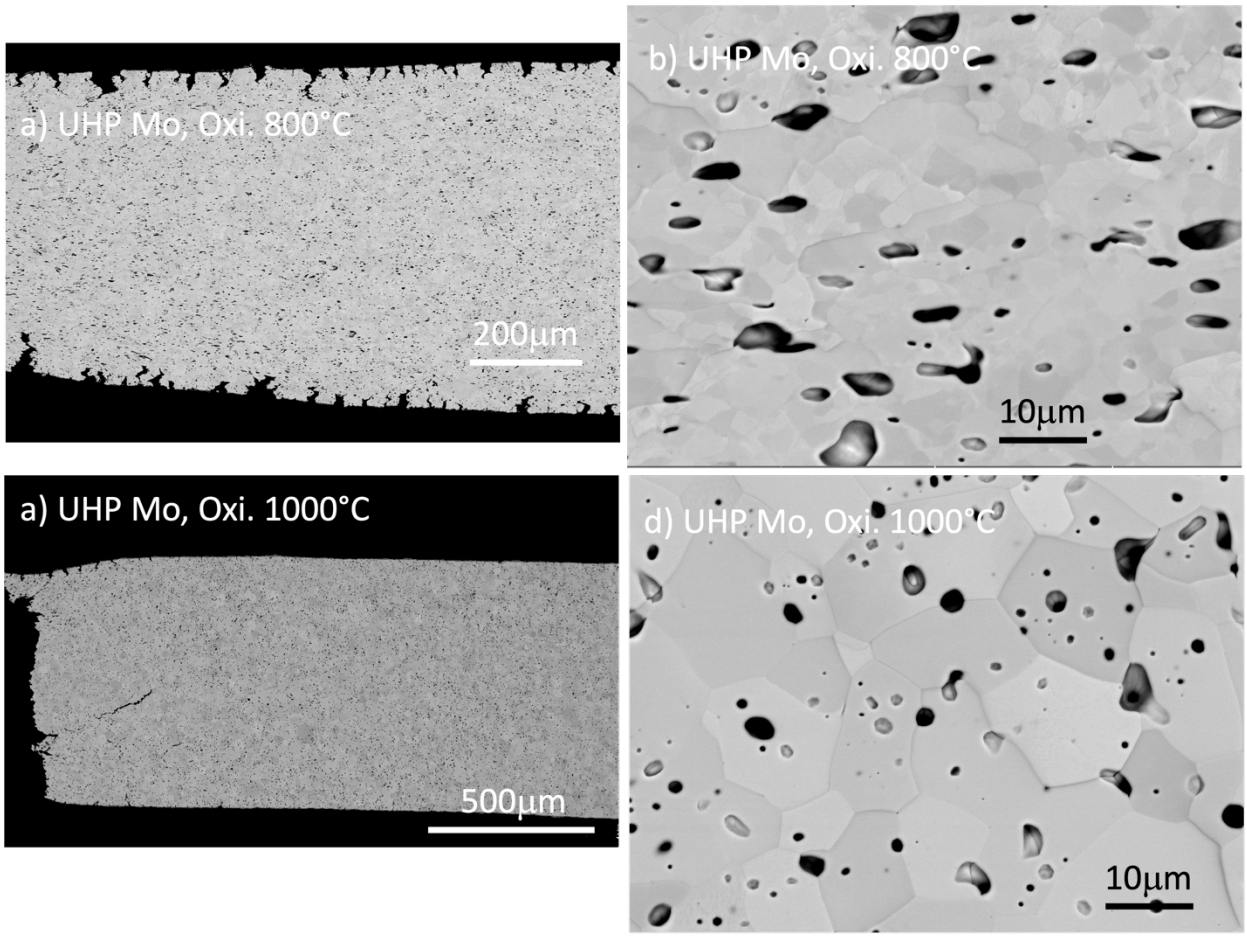

Figure 14: SEM cross-section micrographs of the UHP Mo specimens exposed to He for 100h, a) and b) tested at 800°C, c) and d) tested at 1000°C.

4. CONCLUSION

To support NorthStar's accelerator concept for Mo-99 production, tensile testing at 600-1000°C was conducted on three Mo materials before and after oxidation in UHP He containing less than 5ppm O_2. In the as fabricated condition, enriched aMo disks to be used as Mo target exhibited moderate strength and low ductility at all temperatures due to the presence of voids at grain boundaries leading to intergranular rupture. The non-enriched Mo material fabricated by powder metallurgy (UHP Mo) showed slightly lower strength but superior ductility at 20-1000°C with some specimens exhibiting >30% elongation at rupture. While significant hardening of the material was observed during testing with a mixture of intergranular and transgranular fracture, significant variation in ductility was attributed to microstructure inhomogeneity. The rolled low carbon arc cast Mo used as reference material exhibited much higher strength due to its small grain size and high deformation from the rolling process. A drastic increase in ductility was measured at 1000°C compared to data generated at 20°C-800°C. Oxidation in He at 600°C-1000°C significantly decreased the ductility of the aMo material at all temperatures, likely due to the diffusion and segregation of oxygen at grain boundaries, while no impact was observed on the tensile properties of UHP Mo specimens. Exposure in He resulted in a change in behavior for the rolled Mo at only at 1000°C likely due to the material recrystallization.

5. ACKNOWLEDGEMENTS

The authors would like to thank G. Garner, A. Willoughby, D. Newberry, T. Lowe and K. Epps for their help with specimen preparation, testing and characterization. They also would like to acknowledge H. Hyer, M. Ridley and J. Nash for useful comments on the manuscript. Frequent discussions with the NorthStar's team, in particular A. Ulrich, N. Valluvan and J. Jewell were very helpful and greatly appreciated. This research was sponsored by the U.S. Department of Energy's National Nuclear Security Administration (DOE/NNSA), Office of Material Management and Minimization, Molybdenum-99 Program.

6. REFERENCES

1. P. Richards, W.D. Tucker and S. C. Srivastava, "Technetium-99m: An Historical Perspective", The International Journal of Applied Radiation and Isotopes", 33, 793-799 (1982).
2. National Research Council. 2009. Medical Isotope Production Without Highly Enriched Uranium. Washington, DC: The National Academies Press.
3. T. J. Ruth, "The Shortage of Technetium-99m and Possible Solutions", Annual Review of Nuclear and Particle Science, 70, 77-94 (2020).
4. K.A. Woloshun, G.E. Dale, E.R. Olivas, F.P. Romero, D.A. Dalmas, S. Chemerisov, R. Gromov, R. Lowden, "Thermal Test on Target with Pressed Disks", United States, 10.2172/1245565 (2016).
5. S. Dryepondt, A. Willoughby, B. Johnston, "Oxidation of Molybdenum at 800°C and 1000°C in Flowing He with 0.5 to 250ppm O_2, ORNL report, ORNL/SPR-2022/2490 (2022).
6. C.T. Liu, S.H. Anderson, H. Inouye, "Effect of Oxidizing Environment on Mechanical Properties of Molybdenum and TZM.", ORNL-5431 (1978).
7. E. M. Passmore, "Correlation of Temperature and Grain Size Effects in the Ductile-Brittle Transition of Molybdenum", Philosophical Magazine, 8, 441-450 (1965).
8. S.C. Srivastava and L.L. Seigle, "Solubility and Thermodynamic Properties of Oxygen in Solid Molybdenum", Metallurgical Transaction, 5, 49-52 (1974).
9. K. Leitner, P.J. Felfer, D. Holec, J.Cairney, W. Knabl, A. Lorich, H. Clemens, S. Primig, "On grain boundary segregation in molybdenum materials", Materials and Design 135, 204–212 (2017).
10. A. Kumar and B. L. Eyre, "Grain Boundary Segregation and Intergranular Fracture in Molybdenum", Proceedings of the Royal Society of London. Series A, Mathematical and Physical Sciences, 370, 431-458 (1980).
11. J. B. Brosse, R. Fillit, M. Biscondi, "Intrinsic intergranular Brittleness of Molybdenum", Scripta Metallurgica, 15, 619-623 (1981).
12. S. Tsurekawa, T. Tanaka and H. Yoshinaga, "Grain boundary structure, energy and strength in molybdenum", Materials Science and Engineering, A 176, 341-348 (1994).
13. S.A. Zwonitzer, G.A. Rozak and J.J. Lewandowski, "Effects of rolling temperature and reduction on microstructure and tensile properties of thick plate, powder metallurgy Molybdenum, "Molybdenum and Molybdenum alloys", Edited by A. Crowson et al., The Minerals, Metals and Materials Society, 111-124 (1998).
14. X.J. Yu and K.S. Kumar, "Uniaxial, load-controlled cyclic deformation of recrystallized molybdenum sheet", Materials Science and Engineering A, 540, 187-197 (2012).
15. L. L. Snead, D. T. Hoelzer, M. Rieth and A.A.N. Nemith, "Refractory alloys, Vanadium, Niobium, Molybdenum, Tungsten, Structural Alloys for Nuclear Energy Applications," Edited by G.R, Odette and S.J. Zinkle, 585-640 (2019).

16. S. Dryepondt, A.Willoughby and B. Johnston, “Impact of annealing at 1000°C in flowing He with low O_2 concentration on the room temperature tensile properties of Mo alloys”, ORNL report SPR-2022/2641 (2023).
17. B.V. Cockeram, R.W. Smith and L.L. Snead, "The influence of fast neutron irradiation and irradiation temperature on the tensile properties of wrought LCAC and TZM molybdenum", Journal of Nuclear Materials, 346, 145-164 (2005).